Ordering of the heavy anions in mixed $BaFBr_{0.5}I_{0.5}$ crystals: Experimental results

J. M. Rey, H. Bill,* and H. Hagemann
Département de Chimie Physique, Sciences 2, 30 quai Ernest Ansermet, 1211 Genève 4, Switzerland

F. Kubel
Institute for Chemical Technologies and Analytics, Vienna University of Technology, Getreidemarkt9/164, 1060 Vienna, Austria
(Received 18 July 2005; revised manuscript received 26 August 2005; published 23 November 2005)

Mixed matlokite hosts of composition $BaFBr_xI_{1-x}(0 \leqslant x \leqslant 1)$ (pure and doped with Sm^{2+}, Eu^{2+}) were studied with x-ray crystallography, luminescence, Raman, and electron paramagnetic resonance (EPR) spectroscopy. Results are presented for $BaFBr_{0.5}I_{0.5}$ which demonstrate that a ferrielectric domain structure is formed due to the fact that the heavy halogen ions form separate sublattices with randomly distributed domain walls. The space group of a domain is $P4\,mm$ (No. 99). The EPR data from Eu^{2+} allowed to determine the volume fraction of domains.

DOI: 10.1103/PhysRevB.72.184107 PACS number(s): 61.66.Fn, 77.80.Dj, 61.10.Nz, 78.30.Ly

I. INTRODUCTION

Alkaline-earth fluoro-halides MFX (M=Ca,Sr,Ba, F=Fluorine, and X=Cl, Br, I) are of widespread interest in optics and material sciences; sustained research activity on members of this family is actively ongoing. The main reasons are their model character for structural and lattice dynamics investigations and the fact that (e.g., optically active) rare earth ions (REI) can easily be incorporated. The pure MFX crystallize in the tetragonal matlockite structure ($P4/nmm$, No. 129). Additionally, these materials are of interest because of their potentiality for specific applications. Members of this family containing Sm^{2+} ions were shown to exhibit reversible and stable optical hole burning (OHB) properties at the technologically interesting room temperature.[1–5] Mixed compounds of composition $Ba_{1-y}Sr_yFCl_{1-x}Br_x$ (BaSrFCB in the following) with ($0 \leqslant x,\ y \leqslant 1$) (Ref. 3) ranked among the best OHB performing systems. The BaFBr compound doped with Europium exhibits photostimulated luminescence (PSL).[6–8] This property entailed the application of such systems in imaging screens for two-dimensional x-ray radiography. It was discovered that improved performance of the screens was achieved with mixed compounds $BaFX_{1-x}Y_x:Eu^{2+}$ (X=Cl,Br, Y=Cl,Br,I, $X \neq Y$) doped with Eu^{2+}. Within this general context interest arouses into questions regarding the crystallographic structure of the mixed matlockites. Results concerning $BaFCl_{1-x}Br_x$ and $BaFBr_{1-x}I_x$ were reported (e.g., Refs. 9–14 and others). Contradictions between the published results necessitated, however, to reconsider this matter. The set BaSrFCB behaves regularly[14,15] as expected from randomly decorated lattice sites of the matlockite structure. This means that the heavy anions randomly occupy the two inversion-connected heavy anion lattice sites of the regular matlockite structure. Similar results were published for the family $BaFBr_xI_{1-x}$ with $0<x<1$.[13] Our data from spectroscopic and x-ray diffraction experiments on this latter set showed, however, an unexpected structural behavior which deviates from the published picture. In particular, (a) our Raman spectra showed more than the six lines observed in the pure MFX and in BaSrFCB; (b) Eu^{2+} ions introduced as probes into these hosts produced an electron paramagnetic resonance (EPR) signal dominated by two well-defined tetragonal spectra; (c) single crystal diffraction data showed important anisotropic atomic displacement parameters of the metal and the fluorine ions when the data were resolved in the matlockite (PbFCl) structure. In contrast to the regularly behaving BaSrFCB family, these compounds apparently do not form a "classical" random solid solution on the heavy anion sites. Instead, as will be shown in this paper, a locally ordered, but long-range disordered stacking arrangement of heavy halogen layers presents the most plausible explanation of our experimental data. Figure 1 illustrates this model [see, e.g., also[15,16] for details regarding coordination of the atoms in the matlockite (PbFCl) structure]. To investigate this exceptional situation extended and tightly controlled crystal growth experiments were undertaken and detailed spectroscopic and x-ray diffraction experiments were performed on pure, Sm and/or Eu doped powder samples and single crystals, two structural models, the matlockite (PbFCl) moiety with disorder of the heavy anions (model I) (exemplified by the BaSrFCB family), and a "split model" (model II) were used to interpret our x-ray diffraction data. Both models use the space group $P4/nmm$[129]. This paper essentially pre-

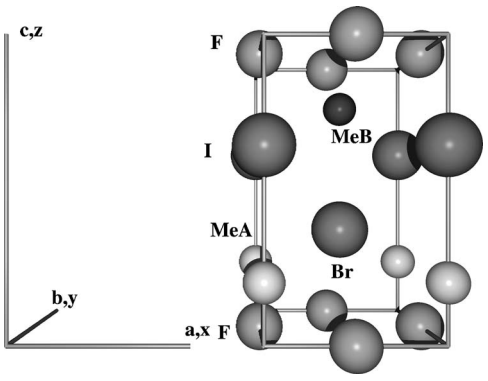

FIG. 1. A unit cell of a domain of $BaFBr_{0.5}I_{0.5}$. Iodine ions form one lattice, bromine ions the other one of the two.

sents the results for $BaFBr_{0.5}I_{0.5}$ as this system shows the effects most clearly. Results of the optical, paramagnetic, and crystallographic investigations are given.

II. EXPERIMENT

Sample preparation. Mixed system samples were either obtained by the pulling method or by slowly cooling the melt (1–5 °C/h), under 0.2 atm of ultrapure argon, under a mixture of Ar/N_2 or a mixture of $Ar(95\%)+H_2(5\%)$. Ultrapure glass-graphite crucibles contained the melt. The synthesis was performed as a two-stage process. Highest purity starting materials BaF_2 (Merck, Suprapur), BaI_2 (Cerac), and $BaBr_2$ (Johnson Matthey) were carefully dried at about 420 K on a high vacuum line. BaFI and BaFBr were precrystallized and subsequently used as the secondary starting material for the preparation of the mixed compounds. Handling, weighting, and loading into the crucibles were performed in an oxygen-free nitrogen atmosphere ($\leqslant$10 ppm of O_2, H_2O) of a Mecaplex glove box. The same procedure was used for the corresponding Sr compounds. Rare earth (RE) impurity doped crystals (concentrations ranging from 10 ppm to 2%) were obtained by introducing the RE ions into the melt during the first step. The stability of the crystals against hydrolysis was tested and no short-term decomposition was observed. High quality single crystals of $BaFBr_{0.5}I_{0.5}$ [typical size $(2-5)\times(1-3)\times 0.5$ mm^3] were selected under a microscope with crossed polarizers from the synthesized batches. One of the samples was oriented by the Laue method. Its best-developed straight borderlines were parallel to the Br-Br, respectively I-I direction of the unit cell (our *a* axis).

For comparison purposes experiments were in addition performed on $BaFBr_{1-x}I_x$ with $x=0.02$, 0.1, 0.2, 0.3, 0.6, 0.8, $BaFCl_{0.5}I_{0.5}$, $SrFBr_{0.5}I_{0.5}$, $SrFCl_{0.5}I_{0.5}$, and the pure hosts BaFI, BaFBr, SrFI, and SrFBr.

X-ray diffraction. The powder samples were obtained by grinding single crystals selected according to the procedure described above. Powder diffraction diagrams were collected on an OMNI diffractometer equipped with a Guinier camera (Cu $K\alpha$ radiation, 5°–90° in 2θ, step 0.02°/60 sec). The single crystal studies used exclusively crystals with sharp optical extinction parallel to the *a* axis. They were mounted on a CAD4 diffractometer [CAD4, Mo $K\alpha$(71.07 pm), scan: $\omega/2\theta$, 300 K]. Diffraction intensities of a whole sphere in the reciprocal space were collected. The powder and single crystal data were reduced with the aid of the Rietveld method.[17]

Optical spectroscopy. The luminescence and Raman experiments were performed on our laboratory-developed computer controlled spectrometer with appropriate low and high temperature Dewars.[18,19] The precision of the polarization states was determined by the light collection system at the entrance of the 1403 Spex double monochromator and the residual nonparallelism of the laser beam ($\approx$5°). Spectra were recorded at temperatures between 10 K and 620 K.

EPR. The spectra at 9.2 GHz were obtained with a laboratory modified *X*-band *E*-line Varian spectrometer whereas the experiments at 36 GHz were realized on a home-built Ka-band spectrometer. Details of the apparatus, data analysis, and computer simulations are described in Refs. 19,20. Both instruments allowed precise sample alignment with the aid of laboratory built goniometers.

TABLE I. The atomic positions of $BaFBr_{0.5}I_{0.5}$. Powder diffraction (data reduction in $P4/nmm$, model I and model II). $T=300$ K. Lattice parameters (pm) $a=b=457.50(9)$, $c=770.89(116)$, and U_{zz}=atomic displacement parameter along *c*.

	x/*a*	*y*/*b*	*z*/*c*	U_{zz}	Pop.
			Model I		
Ba	0.2500	0.2500	0.1829(2)	2.88(10)	1
F	0.7500	0.2500	0.0000	2.836(7)	1
Br	0.2500	0.2500	0.6507(2)	1.39(10)	0.5
I	0.2500	0.2500	0.6507(2)	1.39(10)	0.5
			Model II		
Ba1	0.2500	0.2500	0.1594(8)	1.18(14)	0.5
Ba2	0.2500	0.2500	0.2061(8)	1.18(14)	0.5
F	0.7500	0.2500	0.0000	1.5(4)	1
Br	0.2500	0.2500	0.6501(2)	1.54(9)	0.5
I	0.2500	0.2500	0.6501(2)	1.54(9)	0.5

III. RESULTS

A. Diffraction results on $BaFBr_xI_{1-x}$

Nine different batches of molar fractions $0\leqslant x\leqslant 1$ were at first studied (all at room temperature) to investigate the relation between *x* and the lattice constants. The results demonstrated that *a* varies linearly with increasing iodine content, i.e., Vegard's rule is followed.[13] This information allowed us to determine semiquantitatively the composition of a sample once its lattice constants had been determined. In the following we focus on the systems with bromine to iodine ratios of $x\simeq 0.5$.

Powder diffraction analysis. The diffraction diagrams were at first solved within model I. They revealed no significant deviations from the matlockite structure and no additional reflections. The extinction law $hk0: h+k=2n$ was found to be followed. The probability to have an ordered superstructure was therefore small. But model I yielded an unusually large atomic displacement parameter of Ba along *c* (see Table I) in comparison with this quantity in BaFBr or BaFI. The same data were then analyzed within model II. This resulted in a split position (50%) of the barium with more reasonable atomic displacement parameters of the two sites.

The standardized[17] atomic positions and vibrational parameters obtained on a nominal $BaFBr_{0.5}I_{0.5}$ sample are given in Table I. The powder studies did not allow, however, to distinguish clearly between the two models. In particular, the question of the split fluorines remained unresolved.

Single crystal studies. The selected single crystals (see Sec. II) from several synthesis batches were studied. Diffraction data and conditions of data collection are given in the Appendix (Table VII). The refinement of the collected intensities converged reasonably as shown in this table. The observed diffraction diagram presented no reflections other

TABLE II. The atomic positions and site occupancy for $BaFBr_{1-x}I_x$ crystals [x=0.463(8)]. T=300 K. Lattice parameters (pm): $a=b$=457.23(3), c=769.28(16).

Atom	$BaFBr_{0.537}I_{0.463}$ Wyck	z/c	U (×100)	p
		Model I		
Ba	2c	0.1799(2)	3.12(3)	1
F	2a	0.0	3.6(3)	1
Br	2c	0.6517(2)	1.97(2)	0.63(1)
I	2c	0.6515(2)	1.97(2)	0.37(1)
		Model II		
Ba1	2c	0.1554(2)	1.55(2)	0.5
Ba2	2c	0.2050(1)	1.54(2)	0.5
F	4f	0.0250(9)	1.8(2)	0.5
Br	2c	0.65225(8)	2.9(1)	0.537(8)
I	2c	0.65225(8)	1.76(4)	0.463(8)

than those of the matlockite structure, confirming the absence of any ordered superstructure. Thus, the refinement could be based on one single phase. The composition of different crystals of a same synthesis batch was found to be similar. The data were analyzed with the two models.

Model I: the symmetry was $P4/nmm$ as no further reflections were found. But the atomic displacement factors were again unusually anisotropic for the heavy barium ions, as already observed with the powders. This was also true for the fluorine ions. Model II: split positions of Ba and of F were assumed. The resulting atomic displacement factors for Ba and F were much more reasonable and interatomic distances were close to those of the pure iodine and bromine matlockites. In short, the structure is still tetragonal, an average structure is analyzed for the macroscopic crystal, its space group is $P4/nmm$. Table II gives the results obtained on a sample of composition x=0.463. We investigated crystals through the whole range of x values ($0 \leqslant x \leqslant 1$) and observed ordering throughout. Refinement parameters were obtained for both models at several x values. To reach better insight into the structural features of these systems it was essential to perform optical and EPR spectroscopy on them.

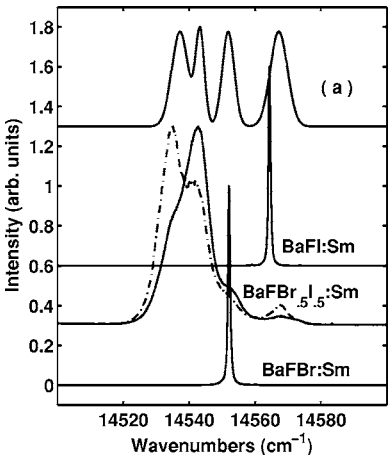

FIG. 2. $^5D_0 \rightarrow {}^7F_0$ emission of $BaFBr_{1-x}I_x:Sm^{2+}$ (x=0, 0.5, 1) at T=77 K. The two lines of the x=0.5 compound are from different regions of the same sample. Excitation at 20 490 cm^{-1}. (a): The four bands resulting from the decomposition of the x=0.5 spectrum. For convenience all four were normalized to 0.5.

TABLE III. Position of the $^5D_0 \rightarrow {}^7F_0$ luminescence of $BaFBr_{1-x}I_x:Sm^{2+}$. T=290 K.

Compound	$^5D_0 \rightarrow {}^7F_0$ (cm^{-1})
BaFBr	14 552
BaFI	14 564
$BaFBr_{0.5}I_{0.5}$	14 568 [a]
	14 551
	14 543
	14 535

[a]Errors: Absolute: ±4 cm^{-1}; relative: ±0.4 cm^{-1}.

B. Luminescence

Luminescence spectra of Sm^{2+} of all the hosts enumerated in Sec. II were recorded. The luminescence transition $^5D_0 \rightarrow {}^7F_0$ of the Sm^{2+} ion was of particular interest as it involves two nondegenerate electronic levels. Figure 2 presents normalized spectra of $BaFBr_{0.5}I_{0.5}$ and of the pure hosts BaFBr and BaFI, all recorded at 77 K. As expected, the pure compounds presented one sharp line whereas the mixed system exhibited a composite structure. The band positions are given in Table III. The spectra of the mixed system present a strikingly better resolved structure in comparison with the results obtained from $BaFBr_xCl_{1-x}:Sm^{2+}(0.1 \leqslant x \leqslant 0.9)$.[12,15] This may be verified in Fig. 3 where the $^5D_0 \rightarrow {}^7F_0$ bands of several $MFX_{0.5}Y_{0.5}$ hosts (M=Ba,Sr and X,Y=Cl,Br,I) are presented–all doped with Sm^{2+}. The spectra labeled 3(a) and 3(b) are well understood.[15] The ones labeled 3(c) and 3(d) are largely independent of temperature. Their detailed analysis showed that the crystals consist of a mixture of

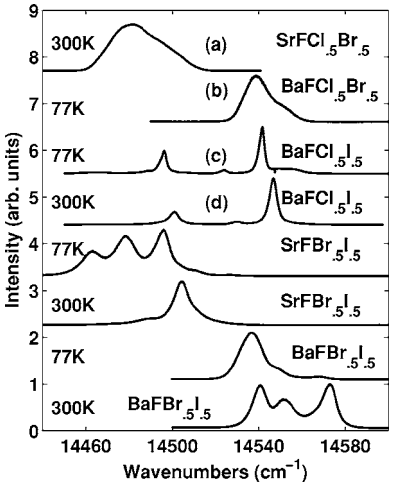

FIG. 3. $^5D_0 \rightarrow {}^7F_0$ emission of $MFX_{0.5}Y_{0.5}:Sm^{2+}$ (M=Sr,Ba; X=Cl,Br; Y=Br,I). T=77/300 K.

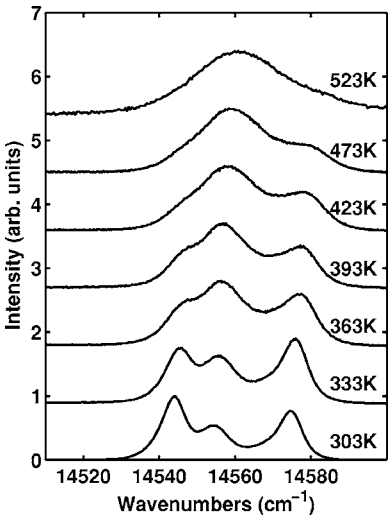

FIG. 4. The temperature dependence of the $^5D_0 \rightarrow {}^7F_0$ emission of $BaFBr_{0.5}I_{0.5}:Sm^{2+}$ at temperatures above 300 K.

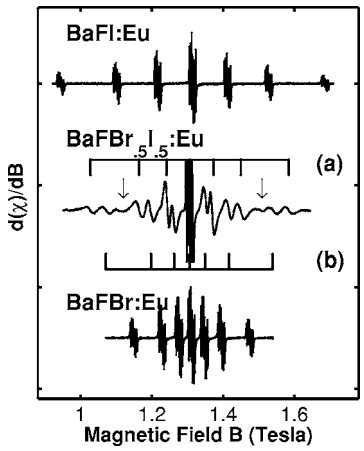

FIG. 5. The Ka-band EPR spectra of $BaFBr_{1-x}I_x:Eu^{2+}$ (x=0, 0.5,1). T=77 K. $B \| c$. The sticks labeled (a) and (b), respectively, point to the two dominant groups of seven fine structure bands in $BaFBr_{0.5}I_{0.5}:Eu$. The arrows label additional bands are not associated with the Eu^{2+} centers (a) and (b).

$BaFCl:Sm^{2+}$ and $BaFI:Sm^{2+}$ crystallites. The positions of the two emission bands are indeed identical to those of the pure crystals. This was further supported by our Raman investigation (see below). The recorded spectra consisted of a superposition of the bands corresponding to pure BaFCl and BaFI matlokites. Finally, the two lowest pairs of spectra of Fig. 3 present a remarkably pronounced temperature dependence between 4.2 and $\cong$270 K. Its origin is of electronic nature as the changes with temperature were "instantaneous" in comparison with the evolution at $T>$RT (see below). This indicates the presence of strongly system- and temperature-dependent nonradiative electronic transitions. The luminescence experiments performed between 300 K and 640 K on $BaFBr_{0.5}I_{0.5}:Sm^{2+}$ showed indeed a different behavior. The four bands observed at room temperature (RT) always coalesced around 640 K into one Lorentzian [with center at 14 560 cm^{-1} and (FWHM) $\approx$ 30.6 cm^{-1}]. When the sample was cooled again to RT the high temperature band shape "persisted" for approximately half an hour, then gradually evolved within approximately 24 h towards the RT spectrum of Fig. 4, often with different relative intensities of the bands. The spatial homogeneity of several $BaFBr_{0.5}I_{0.5}$ samples was examined by luminescence emission. The observed spectra always showed the four bands, but with relative intensities which depended somewhat on the location examined. Luminescence spectra of two different areas of the same sample are presented in Fig. 2. The exact band shape was further sample dependent and also dependent on the excitation wavelengths. An in-depth analysis similar to the one published[15,21] might be performed on the BFBrI set of hosts. This research project is, however, beyond the scope of the present paper.

C. EPR results

Eu^{2+} was introduced into all the hosts enumerated in Sec. II and EPR spectra of all of them were recorded. Its ground state is $^8S_{7/2}$ and the lowest excited electronic states are at energies $\geqslant$24 000 cm^{-1} above the ground state. Figure 5 presents EPR spectra of Eu^{2+} in BaFBr, BaFI and the mixed host $BaFBr_{0.5}I_{0.5}$. They were obtained under identical conditions, in particular with $B \| c$. The spectra consist of patterns of seven fine-structure packets centered around $g \approx 2$. The pure hosts show one pattern indicating the presence of one Eu^{2+} center. Each one of the packets actually consists of two almost fully resolved sextets due to the hyperfine interaction with the two Eu isotopes [^{151}Eu (47.82%) and ^{153}Eu (52.18%), nuclear spin I=5/2]. On the other hand, the dominant part of the spectrum of the mixed host consists of two sets of seven remarkably symmetrical, broad and structureless bands—with the exception of the central one. There are thus two Eu^{2+} centers. The lack of structure is the signature of a distribution of crystal field values centered around a mean value. The central band of the spectrum consists of two resolved sextets, similar to the situation observed in the pure hosts—but with $\approx$20% larger linewidths. The angular variation of the two spectra was studied with $B \| (100)$, (010), and (001) planes and was found to present tetragonal symmetry, with the largest fine structure splitting along $B \| c$. Parametrization was performed with the aid of the spin Hamiltonian [Eq. (1)] of D_{4h} point symmetry by using our procedures published before (Ref. 20).

$$\begin{aligned} H &= H_{Ze} + H_{CF} + H_{hf}^{isot} \\ &= \beta_B g B \cdot S + B_2^0 O_2^0 + B_4^0 O_4^0 + B_6^0 O_6^0 + B_4^4 O_4^4 + B_6^4 O_6^4 \\ &\quad + A_i^{Eu} I_i^{Eu} \cdot S. \end{aligned} \tag{1}$$

The first term of the right-hand side (rhs) is the electronic Zeeman contribution, the last one is the hyperfine interaction with the Eu^{2+} nucleus (isotope i), and the remaining right-hand side part is the Stevens crystal field as defined, e.g., by Refs. 22,23. The results of the fit to the spectra are given in Table IV. The absolute signs of the spin Hamiltonian parameters were determined at 4.2 K sample temperature. The second order crystal field parameter (B_2^0) (Ref. 22) is in all cases the dominant term. This fact together with the large line-

TABLE IV. The spin-Hamiltonian parameters (in 10^{-4} cm^{-1}) for Eu^{2+} in $BaFBr_{1-x}I_x$(x=0,0.5,1). T=78 K.

Compound	$g_{\text{isotropic}}$	B_2^0	B_4^0	B_4^4	B_6^0	B_6^4 [a]
BaFBr	1.992(2)	73(1.0)	0.17(0.03)	0.58(0.18)	0.000(0.002)	0.00(0.02)
BaFI	1.992(2)	177(2)	0.22(0.03)	0.96(0.20)	0.001(0.003)	0.00(0.02)
$BaFBr_{0.5}I_{0.5}$ (a)	1.993(3)	131(5)	0.27(0.05)	1.2(1.0)	0.001(0.002)	–
$BaFBr_{0.5}I_{0.5}$ (b)	1.992(2)	104(5)	0.3(0.05)	1.0(1.0)	0.001(0.002)	–

[a]Orientation of the local EPR axes, see Fig. 1; errors: see text.

widths of the packets only allowed to obtain approximate values of the fourth and sixth order crystal field parameters. The errors given in the tables correspond to the variation needed to double the residual error of the fits. The spectra of Fig. 5 had all been recorded with $B \| c$, the principal axis of the crystal field acting on the Eu ion. Writing down within this situation the matrix of Eq. (1) in the eigenstates of the Zeeman operator $H_{Ze}(H_{Ze} \gg H_{CF} > H_{hf})$ yields that for the central transition (approximately $|7/2\ 1/2\rangle \leftrightarrow |7/2 - 1/2\rangle$) the crystal field only acts in second and higher order. Additionally, the fact that in general the values of the crystal field parameters oberved in the matlockites are rather small compared to $|H_{Ze}|$ (at 36 GHz) implies that this same transition is much less influenced by the crystal field than the other ones for angles $0 \leqslant \varphi \leqslant 45°$ between B and the principal axis of the crystal field. The central packet of the EPR spectrum is therefore only weakly influenced by the crystal field distribution. For this reason the central transitions of the two EPR spectra (a) and (b) practically coincide. This fact will now be used to estimate the fraction of the sum of the two tetragonal Eu^{2+} centers in comparison to all paramagnetic Eu^{2+} centers. Total intensities of the individual bands of the two tetragonal components were obtained from our best K band spectra recorded at 77 K with $B \| c \| C_4$. The digital files were conditioned and integrated twice with the aid of our MATLAB programs. Typical errors were ±12%. The intensities of the corresponding bands of the two spectra were added and normalized by the intensity of the lowest-field pair. The EPR spectra of the pure systems of Fig. 5 were treated in an analogous manner. The following intensity ratios were obtained: for $BaFBr:Eu^{2+}$, 1:1.7 :1.95:2.3; for $BaFI:Eu^{2+}$, 1:1.67:1.92:2.5; and for $BaFBr_{0.5}I_{0.5}:Eu^{2+}$, 1:1.62:1.85:3.8.

As all the systems have the same sign of the dominant crystal field parameter (and of the hyperfine structure constant) the given part of the distribution is significant. The experimental intensity ratios of the pure systems agree very well with those calculated with the aid of our diagonalization and parameter adjustment computer programs. If the two tetragonal Eu^{2+} spectra of the mixed host were the only contributors to the observed EPR spectrum, an intensity distribution close to the ones obtained from Eu^{2+} of the pure hosts would result. Thus, the ratio α=[intensity of the central group of the spectrum of (say) $BaFI:Eu^{2+}$/ intensity of the same quantity of the mixed host] is of interest. If α is not $\simeq 1$ other Eu^{2+} centers contribute which reside at different perturbed regions of the mixed crystal (see below). Concomitantly, their crystal field is a strong function of the perturbed surroundings. As a result their total spectrum is expected to be strongly "spread out" as a function of B, with the exception, however, of their central transition as discussed earlier in this section. This last statement is a working hypothesis as spectra with monoclinic symmetry may contribute in a more complex and individually differing manner. The observed ratio is α=(2.5/3.8), yielding approximately 65%. A number of different local arrangements of the two heavy anions contribute thus to the EPR spectrum of the mixed system, but the two tetragonal sites are clearly much more frequent than expected for a fully disordered crystal. The situation is intermediate between the pure matlockite hosts and the other extreme represented, e.g., by $SrFCl_{0.5}Br_{0.5}$ where a fully disordered heavy anion crystal lattice has been shown to exist[14,15,24] with a total occurrence of tetragonal sites of $\approx$1.9%.

D. Raman results

Factor group (D_{4h}) analysis of the pure matlockites predicts the existence of six first order vibronic Raman transitions transforming as $\Gamma = 2A_{1g} + B_{1g} + 3E_g$ as confirmed by the experiment.[25] The same number of lines was observed in the mixed matlockite moieties (BaSrFCB).[12] Experimental Raman spectra of $BaFBr_{1-x}I_x$ were obtained from crystals of eight compositions ($0 < x < 1$). Figure 6 gives a spectrum of $BaFBr_{0.5}I_{0.5}$ together with the ones of BaFBr, BaFI. Spectra of $BaFBr_{0.5}I_{0.5}$ obtained (at 300 K) with different polariza-

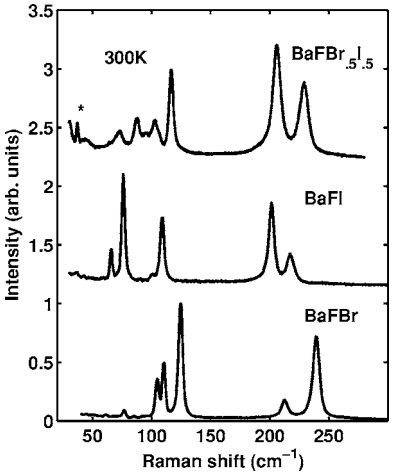

FIG. 6. The Raman transitions of the mixed (x=0.5) and the pure (x=0,1) title compounds. T=300 K. The * designates a laser line.

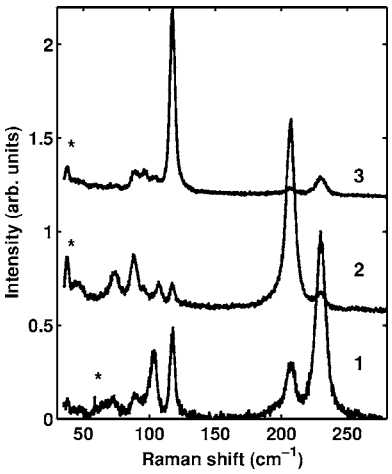

FIG. 7. The Raman transitions of $BaFBr_{0.5}I_{0.5}$. $T=300$ K. 1: $z(ca)x$; 2: $x(aa)x$; 3: $z(cc)z$. The $*$ designates laser lines.

tion geometries are shown in Fig. 7. All the polarizer and analyzer geometries necessary to access the matrix elements of the (symmetrical) polarization tensors were used, but no angular dependence measurements were done. The well-known[25] two group pattern of the spectra of the pure compounds is also observed here (see, e.g., Fig. 6 with one group above $\sim 185\ cm^{-1}$ and the other one below $\sim 140\ cm^{-1}$). The former group consists of two lines at frequencies which shift with composition x. Their linewidths increase for $x \rightarrow 0.5$. At $x=0.5$ the widths are approximately two times larger than the ones at $x=0$ or 1. The line at lower wave number transforms as B_1 and the other one as E. Both are essentially due to fluorine ion lattice motion.

TABLE V. First order Raman transitions of BaFBr, BaFI, and $BaFBr_{0.5}I_{0.5}$.

Host	$A_1(te1)$	$B_1(te2)$	$E_g(te3)$	T (K)	Remarks[a]
BaFBr	122.2	210.5	237.3	300	[b]
	102.0		108.0		
			74.2		
BaFI	102	202.6	218.2	300	[c]
	77.4		110		
			66.6		
$BaFBr_{0.5}I_{0.5}$	118.0	207.3	230.3	300	[d]
	107.4		104.2		
	96.6		73.9		
	89.2		45.5		
$BaFBr_{0.5}I_{0.5}$	120.6	210.5	233.6	80	[d]
	106.4		104.7		
	98.6		73		
	90.9		48.9		

[a]$(te1)=x(aa)x,z(cc)z$; $(te2)=x(aa)x$; $(te3)=z(ca)x$ in the notation of Porto. Errors: $\pm 0.8\ cm^{-1}$.
[b]Reference 25.
[c]Reference 16.
[d]This paper. Values were obtained from Stokes and anti-Stokes spectra.

The low frequency group of the mixed crystal differs in an important way from the one of the pure hosts as it presents clearly more than four lines. The positions and the experimentally obtained symmetry species of the identified transitions are given in Table V. A very weak band seen between 300 and 320 cm^{-1} as well as features between 40 and 70 cm^{-1} were not included as their identification is not fully ascertained. Some of the observed extinctions are less than what our Raman spectrometer allows for. Its valid polarization properties had been verified with the aid of a single crystal of SrFCl oriented by x-ray Laue technique. There is further a scattering geometry-dependent change in the linewidths of the 73.9 and the 88.8 cm^{-1} bands and the one at 118 cm^{-1} presents an asymmetrical shape. But no clearcut coupling with polar phonons longitudinal-optical transverse-optical (LO-TO splitting) could be established. It would indeed be very useful to perform far infrared experiments on these samples. Coupling to polar vibrations of the crystal may indeed contribute to the deviating polarization properties. But the existence of internal domain walls (see Sec. IV) may contribute in scrambling the polarization state of the Raman laser. We found indeed, that the quality of the extinctions depended on the samples used. The temperature dependence of the lines was further studied. Between 4.2 and 290 K essentially conventional temperature effects (shift of the band positions and changed band widths, see above) were found. But experiments performed between 340 and 550 K showed a gradual conversion of the spectrum into the one (at the highest temperatures reached) of a "normal" mixed matlockite with five resolved bands. The general behavior under thermal cycling of the Raman response was similar to the one of the luminescence spectra.

IV. DISCUSSION

The luminescence and Raman results presented in Sec. III demonstrate that $BaFBr_{0.5}I_{0.5}$ undergoes an order-disorder phase transition during heating to above RT. The high temperature phase is isostructural with the one observed at all temperatures in the "normal" mixed matlockites (e.g., $BaFBr_{0.5}Cl_{0.5}$).[15] The low temperature phase is ordered as the following arguments show. The x-ray diffraction results yielded the space group $P4/nmm$ for $BaFBr_{0.5}I_{0.5}$. But both the EPR and Raman data do not back the model of the "normal" mixed matlockite structure which implies the existence of the two inversion-connected heavy ion lattices being occupied randomly (i.e., with probability 1/2 for the $x=0.5$ composition) by Br and I, respectively.[15] The vibrations at the Γ point of these latter crystal structures presented a one mode behavior[26,27] as their Raman spectrum consisted of six bands. This was observed at all temperatures investigated (35–300 K) similar to the situation of the pure hosts (but with increased linewidths). The Raman spectrum of $BaFBr_{0.5}I_{0.5}$ presents at least nine, probably more, Raman bands, in blatant disagreement with this one mode model. A second piece of evidence of a nonstatistical distribution of Br, I is given by the EPR results. Two dominant tetragonal contributions of similar intensity were found (see Sec. III C), whereas the system $BaFBr_{0.5}Cl_{0.5}:Eu^{2+}$ presents a multitude

TABLE VI. The irreducible representations (IREPS) of the C_{4v}^1 subgroup of the matlockite structure.

Ion	Wykoff site	Site symmetry	IREPS
Ba1	1*b*	4 mm	A_1+E
Ba2	1*a*	4 mm	A_1+E
F	2*c*	2 mm	A_1+B_1+2E
Br	1*a* (1*b*)	4 mm	A_1+E
I	1*b* (1*a*)	4 mm	A_1+E
Zone center phonon modes			
Total	$\Gamma=5A_1+B_1+6E$		
Raman/infrared	$\Gamma=4A_1+B_1+5E$		

of broad and, for the most part, ill-resolved features of low symmetry.[24] For these reasons we admit that the two heavy anion sites in the unit cell are not randomly decorated. Instead, they form different lattices. One of them is occupied by Br ions and the other one by I ions (see Fig. 1). This structure preserves tetragonal symmetry but without the inversion center which is part of the D_{4h} factor group of $P4/nmm$. The crystallographic subgroup which is "translationsgleich" but with a factor group without inversion is the symmorphic space group $P4\ mm$ (No. 99).[28] It is thus natural to discuss the observed properties of the $BaFBr_{0.5}I_{0.5}$ compound with the aid of this latter space group. By using the tables of Rousseau *et al.*,[29] the irreducible representations of the zone center phonons were obtained, as given in Table VI. Ten regular Raman bands are predicted by this model, in good agreement with the experiment. This structural model implies the existence of two different Ba sites in the unit cell. One is associated with a nearest iodine neighbor along the *z* axis and the other with a bromine one (see Fig. 1). Both have C_{4v} site symmetry. When identical probabilities are admitted for the Eu^{2+} impurity to occupy the two barium sites, then two tetragonal EPR spectra of equal intensity are expected. In our best samples this is indeed the case within experimental precision. The model further implies different *z* coordinates for Br and I, respectively. The unit cell has a resulting electric dipole moment along *z* due to the fact that the sites Ba1 and Ba2 are no longer connected by inversion. Any portion of this structure is thus a ferrielectric domain as the total polarization is due to the action of two mutually only partially compensating dipoles of the unit cell. To the best of our knowledge, no direct determination of the dielectric properties of this system has been published. We thus have only indirect indications regarding reversal of the polarization. Figure 4 shows that the fluorescence emission bands of the Sm^{2+} ion coalesce into one at around 520 K. And our Raman experiments demonstrated that the spectrum coalesced into a five line structure (see Sec. III D) at the same temperature. This indicates that the heavy anion order disappeared due to randomization of the occupation of the corresponding two lattices. Therefore, around 520 K the crystal structure of the domain goes over into the "normal" mixed matlockite structure described before. The low temperature situation was obtained again (note the delays, see Sec. III D) after recooling the sample to RT. It is thus likely that both possible polarization orientations of a given domain are accessible when cooling a sample exposed to a suitable electric field from above 500 K to RT.

The luminescence data as well as the results of the EPR analysis show that the crystals do not form one single domain. The domain walls most likely consist of single or multiple layers of the pure species BaFBr or BaFI. A stacking sequence along the *c* axis of the form …*ABABBABABAB*…, respectively, …*ABABBBBABA*., etc., will result. The Sm^{2+} ions located in such a wall will be subjected to a crystal field approaching values of the pure hosts and with a broad probability distribution due to the fact that the thickness and the disposition of the walls is random. Indeed, as seen, e.g., in Fig. 2, two emission bands are centered near the region of the lines of the pure hosts but they have a considerable linewidth, whereas the other two bands arise from Sm^{2+} ions occupying the two barium positions inside of a given domain. The "normal," disordered, mixed matlockites present, instead, a wide luminescence band almost without structure as shown, e.g., in Figs. 3(a) and 3(b). The fact that the domain walls are not of uniform thickness is further supported by the EPR results. Spectrum (b) of Fig. 5 does not exhibit any clearcut Eu^{2+} spectrum of the pure compounds, though a fraction of the order of 30–40 % of a typical sample consists of perturbed regions. A further complication arises from the fact that, probably, the domain walls do most likely not extend over the whole of the cross section of a macroscopic sample. Indeed, walls between adjacent walls at the same *z* axis coordinate, or nearly so, are expected. Remarkably, the system does not separate into two phases as is for instance observed for $SrFCl_{0.5}I_{0.5}$ nor does it form a disordered structure.

We do not have enough data on $SrFBr_{0.5}I_{0.5}$ to be able to conclude definitely about the structural model of this host, but those available tend to show that similar ordering exists also there. The large nuclear charge and the sizable relativistic effects of iodine have important effects on the electronic structure description and a detailed band structure calculation of this system would be extremely helpful as this would allow to determine the importance of covalency involved in the I-I bond ordering within the iodine planes. Further, detailed band structure information would allow to investigate the relation between the band order and geometrical structure of the unit cell. Additionally, this might bring information about the polarization effects between the adjacent iodine and bromine planes as the two anion species have different electronegativity.

The deviating structural and dielectric behavior of $BaFBr_{0.5}I_{0.5}$ within the matlockite family is remarkable, indeed. The results obtained may further allow us to bring more insight into the mechanism(s) of charge storage of PSL.

V. CONCLUSIONS

Our spectroscopic and x-ray data allowed us to show that $BaFBr_{0.5}I_{0.5}$ forms an ordered structure as bromine and iodine occupy one, respectively, the other one, of the two

TABLE VII. The conditions of data collection and refinement for $BaFBr_{1-x}I_x$ powder ($x=0.5$) and crystal [$x=0.463(8)$]. $T=291$ K.

Factor	Model 1	Model 2
	Powder $BaFBr_{0.5}I_{0.5}$	
R_p	4.1	3.9
R_{pw}	5.4	5.2
R_{exp}	2.5	2.5
S	2.2	2.1
	Single crystal $BaFBr_{0.537}I_{0.463}$[a]	
Refinement		
Space group	$P4/nmm$[129]	$P4/nmm$[129]
$R(R_w)$	0.0643(0.076)	0.033(032)
Parameters	11	18
Goodness of fit	5.31	2.25

[a]Reflections measured: 4928, independent reflections: 752. R_{int}: 0.064, reflections with $I>3\sigma(I)$:546. Volume ($\times 10^6$ pm^3)V =160.83(4). Density (gr/cm^3)d=5.328.

inversion-connected heavy anion lattices of the parent matlockite structure. In spite of the fact that the x-ray data of macroscopic samples are interpreted within the matlockite structure $P4/nmm$, the spectroscopic results show that a $P4mm$ unit cell has to be adopted. The system is ferrielectric. But a lack of data does not allow us to give information on the magnitude of the polarization, save that the magnitude may be rather small as there were no striking effects observed in the Raman spectra.

ACKNOWLEDGMENTS

This research was supported by the Swiss National Science Foundation (Grant No. 21-50828.97). We thank the SNF for this contribution. The authors thank D. Lovy for programming contributions. H. B. thanks Professor Andreas Bill for a helpful discussion.

APPENDIX: BACKGROUND MATERIAL REGARDING X-RAY DIFFRACTION DATA COLLECTION

Table VII shows the parameters characterizing the data acquisition.

*Electronic address: hans.bill@chiphy.unige.ch

[1] W. E. Moerner, Persistent Spectral Hole Burning: Science and Applications, *Topics in Current Physics* (Springer, Berlin, Heidelberg, 1988). Vol. 44.
[2] R. Macfarlane, J. Lumin. **100**, 1 (2002).
[3] R. Jaaniso and H. Bill, Europhys. Lett. **16**, 569 (1991).
[4] J. Zhang, S. Huang, and J. Yu, Opt. Lett. **17**, 1146 (1992).
[5] K. Holliday, C. Wei, M. Croci, and U. P. Wild, J. Lumin. **53**, 227 (1992).
[6] L. H. Brixner, Mater. Chem. Phys. **16**, 213 (1987).
[7] T. Hangleitner, T. K. Koschnick, J.-M. Spaeth, R. H. D. Nuttall, and R. S. Eachus, J. Phys.: Condens. Matter **2**, 6837 (1990).
[8] G. Blasse, J. Alloys Compd. **192**, 17 (1993).
[9] A. Bergman and G. Bukhalova, Zh. Obshch. Khim. **19**, 603 (1949).
[10] L. Jiauhua and S. Niazeng, Gaodeng Xuexiao Huaxue Xuebao **6**, 957 (1985).
[11] S. Hodorowicz, E. Hodorowicz, and H. Eick, Cryst. Res. Technol. **19**, 1377 (1984).
[12] R. Jaaniso, H. Hagemann, F. Kubel, and H. Bill, Chimia **46**, 133 (1992).
[13] S. Ruan, M.-W. Wang, J. Du, and M.-Z. Su, J. Alloys Compd. **249**, 234 (1997).
[14] H. Hagemann, P. Tissot, D. Lovy, F. Kubel, and H. Bill, J. Therm Anal. Calorim. **57**, 193 (1999).
[15] R. Jaaniso, H. Hagemann, and H. Bill, J. Chem. Phys. **101**, 10323 (1994).
[16] D. Nicollin and H. Bill, J. Phys. C **11**, 4803 (1978).
[17] L. M. Gelato and E. Parth, J. Appl. Crystallogr. **20**, 139 (1987).
[18] A. Monnier, Thesis No. 2491, University of Geneva, 1992.
[19] J. M. Rey, Thesis No. 3189, University of Geneva, 2000.
[20] J. M. Rey, H. Bill, D. Lovy, and H. Hagemann, J. Alloys Compd. **274**, 164 (1998).
[21] R. Jaaniso and H. Bill, J. Lumin. **64**, 173 (1995).
[22] T. Hutchings, of *Solid State Physics* (McGrawHill, 1964). Vol. 16.
[23] A. Abragam and B. Bleaney, *Electron Paramagnetic Resonance of Transition Metal Ions* (Clarendon Press, Oxford, 1970).
[24] F. Constantin, D. Lovy, and H. Bill, (unpublished).
[25] J. F. Scott, J. Chem. Phys. **49**, 2766 (1968).
[26] S. G. Yu, K. W. Kim, L. Bergman, M. Dutta, M. A. Stroscio, and J. M. Zavada, Phys. Rev. B **58**, 15283 (1998).
[27] A. P. Ayala, C. W. A. Paschoal, J. Guedes, W. Paraguassu, P. C. Freire, J. Mendes-Filfop, R. L. Moreira, and J.-Y. Gesland, Phys. Rev. B **66**, 214105 (2002).
[28] *International Tables for Crystallography*, (D. Reidel, Dordrecht 1983). Vol. A.
[29] D. Rousseau, R. Bauman, and S. Porto, J. Raman Spectrosc. **10**, 253 (1981).